HHS Public Access

Author manuscript

Mol Cell. Author manuscript; available in PMC 2017 September 01.

Published in final edited form as:

Mol Cell. 2016 September 1; 63(5): 753–767. doi:10.1016/j.molcel.2016.07.014.

Post-transcriptional regulation of glycoprotein quality control in the endoplasmic reticulum is controlled by the E2 Ub-conjugating enzyme UBC6e

Masatoshi Hagiwara[1], **Jingjing Ling**[1], **Paul-Albert Koenig**[1,2], and **Hidde L. Ploegh**[1,3,*]

[1]Whitehead Institute for Biomedical Research, Cambridge, MA 02142

[3]Department of Biology, Massachusetts Institute of Technology, Cambridge, MA 02142

Abstract

Endoplasmic reticulum-associated degradation (ERAD) is essential for protein quality control in the ER, not only when the ER is stressed, but also at steady state. We report a new layer of homeostatic control, in which ERAD activity itself is regulated post-transcriptionally and independently of the unfolded protein response by adjusting the endogenous levels of EDEM1, OS-9 and SEL1L (ERAD enhancers). Functional UBC6e requires its precise location in the ER to form a supramolecular complex with Derlin2. This complex targets ERAD enhancers for degradation, a function that depends on UBC6e's enzymatic activity. Ablation of UBC6e causes up-regulation of active ERAD enhancers and so increases clearance not only of terminally misfolded substrates, but also of wild-type glycoproteins that fold comparatively slowly *in vitro* and *in vivo*. The levels of proteins that comprise the ERAD machinery are thus carefully tuned and adjusted to prevailing needs.

Graphical abstract

*Correspondence: ploegh@wi.mit.edu.

[2]Present address: Klinikum rechts der Isar, Technische Universität München, Institut für Klinische Chemie und Pathobiochemie, 81675 München, Germany

Supplemental Information: Supplemental information including Supplemental Experimental Procedures, 11 Suppelemental Figures and 1 Table can be found with this article online.

Author Contributions: M.H. designed and performed most of experiments and generated cell lines; J.L. performed some *in vitro* experiments and generated several cell lines and constructed various plasmids; P.A.K generated UBC6e knockout mice, MEF cells and constructed various plasmids; M.H., J.L. and H.L.P. wrote the manuscript and all authors edited and approved the manuscript.

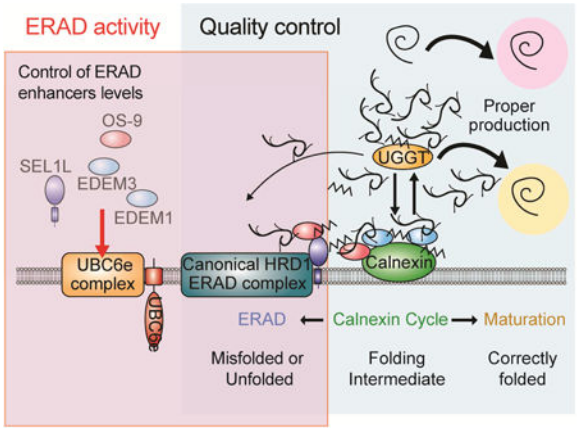

Introduction

The endoplasmic reticulum (ER) is the cellular compartment where membrane and secretory proteins are synthesized. Together, these comprise ~30% of the cellular proteome (Palade, 1975). In the ER, these proteins mature and undergo co- and post-translational modifications. Strict quality control is imposed on newly synthesized proteins, such that only correctly folded proteins are released to their final destination. Misfolded or unfolded proteins are distinguished from correctly folded proteins by the ER-resident quality control apparatus. Proteins that fail to fold correctly are then segregated from correctly folded proteins: the latter can traverse the secretory pathway. Misfolded proteins may be directed to the cytosol by means of a protein-conducting complex, also called the dislocon (Smith et al., 2011). Upon transfer to the cytosol, aberrant proteins are degraded by the ubiquitin-proteasome system. The combined action of the sensors that recognize misfolded proteins, and the dislocon with its connections to the ubiquitin-proteasome system, executes what is now known as ER associated degradation (ERAD).

For N-linked glycoproteins, their glycans play an important role in monitoring and controlling folding status (Xu and Ng, 2015). The ER contains a number of lectins, each of which recognizes and discriminates among specific N-linked glycans. Calnexin (CNX) and calreticulin (CRT), lectin chaperones that recognize the G_1Man_9 (where G is Glucose and Man is Mannose) form of N-linked glycans, promote productive folding in complex with the oxidoreductase ERp57 (Ellgaard and Frickel, 2003)., Interactions of newly synthesized glycoproteins with EDEM-family proteins (EDEM1, EDEM2 and EDEM3), lectins with mannosidase activity, are diagnostic of incompletely folded, or misfolded, N-linked glycoproteins. Overexpression of any of the EDEM family proteins eliminates the lag phase often seen in the degradation of glycoprotein ERAD substrates (Hirao et al., 2006; Hosokawa et al., 2001; Olivari et al., 2005). This lag phase results from attempts at productive folding in the course of the CNX cycle. Elimination of the lag phase by overexpression of EDEM family proteins accelerates ERAD, attributable to premature release of ERAD substrates from CNX, assisted by the mannosidase activity of EDEM-family proteins (Molinari, 2003; Oda, 2003). OS-9 is a lectin with a mannose 6-phosphate receptor homology (MRH) domain that can bind to terminally misfolded glycoproteins in

which the N-glycans have been trimmed to the Man_{5-7} form by EDEM-family proteins or by ER mannosidase 1 (Satoh et al., 2010). SEL1L receives terminally misfolded proteins through a hand-off from lectins that include EDEM1 and OS-9 (Christianson et al., 2008; Cormier et al., 2009) and serves as a scaffold protein for a major ERAD component, the HRD1 complex, which establishes a functional connection with the cytoplasmic ubiquitin-proteasome system (Iida et al., 2011).

The ER resolves stress, as caused by accumulation of aberrant proteins, via induction of the unfolded protein response (UPR) to maintain protein homeostasis. EDEM-family proteins, OS-9 and SEL1L transcripts are upregulated in the course of the UPR, a pathway activated by ER stressors such as tunicamycin, dithiothreitol (DTT) or thapsigargin. Such stress leads to accelerated ERAD of misfolded or unfolded substrate proteins (Yoshida et al., 2003). At steady state, EDEM1, OS-9 and SEL1L have relatively short half-lives (1-2 hours) (Mueller et al., 2006; Reggiori et al., 2010). It was suggested that EDEM1 and OS-9 undergo lysosomal degradation upon exit from the ER and segregation into the secretory pathway for delivery to endosomal compartments (Reggiori et al., 2010), but specific mechanisms of protein recognition and degradation remain unresolved. Likewise, the factor(s) that contribute(s) to the short half-lives of ERAD enhancers are unknown.

UBC6e is an E2 ubiquitin conjugating enzyme that localizes to the ER via its tail-anchor. We identified UBC6e as a protein that interacts with SEL1L, and thus is a component of the larger HRD1 ERAD complex. (Figure 1A) (Mueller et al., 2008). A reduction in the expression of UBC6e impaired degradation of endogenous Class I MHC heavy chains (Burr et al., 2011). UBC6e also forms a complex with RMA1, an ER-resident E3 ligase distinct from the Hrd1 complex, and Derlin1, hypothesized to be a component of the dislocon (Lilley and Ploegh, 2004). This complex has been suggested to regulate degradation of CFTRΔ508, a commonly used ERAD substrate (Younger et al., 2006). Mouse embryo fibroblasts (MEFs) generated from UBC6e knockout mice show an accumulation of EDEM1, OS-9 and SEL1L, suggesting a possible role for UBC6e in controlling ERAD capacity. $UBC6e^{-/-}$ mice suffer from male sterility and auditory defects. The molecular causes for these defects remain to be identified (Koenig et al., 2014).

Here we demonstrate that UBC6e down-regulates EDEM1, EDEM3, OS-9 and SEL1L (ERAD enhancers) in the absence of ER stress. UBC6e's function depends strictly on its E2 enzymatic activity but not its phosphorylation status. The exact ER membrane localization of UBC6e and the supramolecular complexes in which UBC6e participates determine its activity, and directly control the levels of components essential for ERAD activity. The absence of UBC6e increases the levels of ERAD enhancers with a corresponding increase in the rate of clearance of misfolded and/or incompletely folded substrates. $UBC6e^{-/-}$ MEFs show accelerated mannose trimming and premature substrate release from CNX, initiated by ER mannosidase-dependent eviction of substrate from the CNX cycle. Finally, by deletion of UBC6e, accelerated degradation is observed in tissue culture and *in vivo*, not only for canonical ERAD substrates, but also for folding intermediates of proteins that fold slowly, such as tyrosinase. ERAD activity is curtailed under normal circumstances to balance productive folding and degradation of native proteins to avoid the loss-of-function due to premature degradation of proteins that fold comparatively slowly.

Results

EDEM1, OS-9 and Sel1L enhance ERAD and are upregulated post-transcriptionally in UBC6e$^{-/-}$ cells, independently of the UPR

The HRD1 complex is a multi-subunit protein complex involved in retro-translocation of misfolded proteins from the ER to the cytosol (Stein et al., 2014). The complex contains UBC6e, presumed to act as its cognate E2 ubiquitin conjugating enzyme. It further contains Derlin1/2/3, VIMP, UBXD8, EDEM1, OS-9.1/.2 and XTP3B (Figure 1A) (Koenig and Ploegh, 2014) but an accurate definition of its composition remains a challenge, because of the possible existence of sub-complexes. In UBC6e$^{-/-}$ mice and their derived embryonic fibroblast (MEF) lines, we observed up-regulation of select components of the HRD1 ERAD complex, including EDEM1, OS-9 and SEL1L (Figure 1B). This up-regulation can be reversed by reintroduction of wild-type UBC6e, not only when UBC6e is expressed constitutively (Figure 1F) but also when induced for 24 h off a doxycycline-inducible promoter (Figure 4B). Deletion of UBC6e does not affect the level of the homologous E2, UBC6 (Figure 1B). The observed restoration of ERAD enhancer levels is therefore specific for UBC6e. Notwithstanding the increase in ERAD enhancers over the course of the UPR, RNA-seq data showed no obvious changes in transcript levels for ERAD enhancers (Figure 1D and S1). Their protein levels must therefore be regulated post-transcriptionally. We assessed the levels of BiP, Grp170 and P5 as signature indicators of UPR activity and observed no changes (Figure 1E). The levels of ERAD enhancers in UBC6e$^{-/-}$ cells are thus regulated independently of the UPR.

Homeostasis of SEL1L, EDEM1 and OS-9 requires enzymatic activity of UBC6e

UBC6e is class III ubiquitin-conjugating (E2) enzyme, C-terminally tail-anchored in the ER membrane (van Wijk and Timmers, 2010). We investigated the contribution of its catalytic activity and phosphorylation status to the observed increase in ERAD enhancer levels in Ub6e$^{-/-}$ cells. We eliminated the enzymatic activity of UBC6e by mutation of its E2 catalytic cysteine C91S (Lenk et al., 2002). We also mutated the single known phosphorylation site (Menon et al., 2013) in UBC6e by generating a S184A variant. We also created a phospho-mimetic variant, S184E (Figure 1C). Both S184A and S184E mutants down-regulated ERAD enhancers as efficiently as did wild-type UBC6e, whereas the C91S mutant did not (Figure 1F). E2 activity of UBC6e is thus essential for attenuation of ERAD enhancers.

UBC6e$^{-/-}$ cells show elevated ERAD activity

UBC6e$^{-/-}$ cells up-regulate ERAD enhancers selectively. Because UBC6e participates in quality control in the ER, we hypothesized that deletion of UBC6e might attenuate degradation of ERAD substrates, including misfolded EDEM1, OS-9 and SEL1L. However, the observed selective up-regulation of ERAD enhancers in UBC6e$^{-/-}$ cells without UPR led us to consider an alternative possibility, namely that under normal conditions ERAD enhancers are actively degraded in a UBC6e-dependent manner to regulate their participation in ERAD.

We first confirmed by immunofluorescence that excess ERAD enhancers produced in UBC6e$^{-/-}$ cells are localized correctly. We saw no significant changes in their localization

and did not note formation of any aggregates (Figure 2A). We then tested the activity of ERAD in wild-type and UBC6e$^{-/-}$ cells by transfecting them with a model ERAD substrate, null Hong Kong (NHK), a variant of the glycoprotein α1-antitrypsin bearing a frameshift mutation that causes a C-terminal truncation of 61 amino acids (Sifers et al., 1988). Indeed, degradation of NHK was accelerated in UBC6e$^{-/-}$ cells ($t_{1/2}$ > 120 min in wild-type cells, $t_{1/2}$~80min in UBC6e$^{-/-}$ cells; Figure 2B). Addition of the proteasome inhibitor ZL_3VS blocked the degradation of NHK in both cell lines. The UBC6e loss-of-function mutation thus produces a gain-of-function with respect to ERAD activity (Figure 2B). We confirmed that the observed increase in ERAD activity applied also to another model ERAD substrate, RI332. RI332 is a truncated variant of the type I ER transmembrane glycoprotein ribophorin (RI), containing only the N-terminal 332 amino acids of its luminal domain (Tsao et al., 1992). We observed acceleration in the rate of degradation of RI332 in UBC6e$^{-/-}$ cells ($t_{1/2}$ > 60 min in wild-type cells, $t_{1/2}$~45min in UBC6e$^{-/-}$ cells; Figure 2C). Excess ERAD enhancers produced in UBC6e$^{-/-}$ cells must therefore be folded correctly and functional. Conversely, UBC6e is likely involved in a pathway that -in the absence of obvious stressors- continually degrades otherwise functional ERAD enhancers to control their levels, and therefore should be considered an ERAD rheostat.

Increased ERAD activity is initiated by early mannose trimming of NHK

We focused on identifying the underlying mechanism for increased ERAD activity in UBC6e$^{-/-}$ cells. In pulse-chase experiments in UBC6e$^{-/-}$ cells, we observed a subtle increase in the mobility of NHK at later chase periods, as monitored by SDS-PAGE, in comparison with NHK retrieved from wild-type cells (Figure 2B). We repeated the pulse-chase in UBC6e$^{-/-}$ cells rescued with either wild-type or C91S UBC6e. At the 3-hour time point, NHK showed a noticeable increase in mobility in UBC6e$^{-/-}$ cells compared to wild-type cells. Stable expression of wild-type UBC6e reverts this phenotype, but the catalytically inactive mutant C91S does not. The observed differences in electrophoretic mobility of NHK are therefore UBC6e-dependent (Figure 2D). The observed increase in mobility of NHK must be due to increased mannose trimming of N-glycans on NHK. In fact, treatment with an α-mannosidase I selective inhibitor, kifunensine, eliminates both the mobility shift observed for NHK and the difference in rates of degradation of NHK in wild-type and UBC6e$^{-/-}$ cells (Figure 2E). Among EDEM family proteins, EDEM1 and EDEM3 but not EDEM2 are up-regulated in an UBC6e-dependent manner, suggesting that they are responsible for the increased mannose trimming in UBC6e$^{-/-}$ cells (Figure 2F).

Early mannose trimming leads to premature release of NHK from Calnexin (CNX)

In a pulse-chase experiment, wild-type cells degrade NHK more slowly during the first hour of chase than do UBC6e$^{-/-}$ cells (Figure 2B). This lag phase has been associated with the operation of the calnexin (CNX) / calreticulin (CRT) cycle (Molinari, 2003; Oda, 2003). CNX binds to the G_1Man_9 form of N-glycans on folding intermediates and facilitates productive folding by formation of a complex with the oxidoreductase ERp57. Removal of the innermost glucose from G_1Man_9 by glucosidase II releases the substrate from CNX. (UDP)-glucose: glycoprotein glucosyl transferase (UGGT) senses the folding status of glycoprotein substrates. UGGT monoglucosylates incompletely folded substrates to create the G_1Man_9 form of N-glycans, which then allows the substrate an additional round of the

CNX/CRT cycle. If folding is incomplete even after several attempts, terminally misfolded or unfolded substrates undergo further trimming of mannose, which then directs the substrate to the ERAD pathway.

We transfected wild-type and UBC6e$^{-/-}$ cells with NHK and then retrieved CNX by immunoprecipitation. We observed faster release of NHK from CNX in UBC6e$^{-/-}$ cells than in wild-type controls. Time of release corresponded with that observed for the lag phase that precedes degradation in wild-type cells (Figure 3A and S2A). In UBC6e$^{-/-}$ cells, we observed faster electrophoretic mobility of NHK, which we attribute to mannose trimming. This phenotype is reversed by re-introduction of wild-type UBC6e, but not the C91S mutant (Figure 3B and S2B). To the best of our knowledge, this is the first time that mannose trimming has been observed on protein substrates bound to CNX.

In UBC6e$^{-/-}$ cells, ERAD substrates are quickly handed over from the CNX cycle to the ERAD pathway

EDEM1, EDEM3, OS-9 and SEL1L are all up-regulated in UBC6e$^{-/-}$ cells, leading to a corresponding increase in functional interactions. More EDEM1, EDEM3 and OS-9 were recovered in association with CNX in UBC6e$^{-/-}$ cells than in wild-type cells (Figure 3C). In similar fashion we observed increased interactions between SEL1L and OS-9 (Figure 3D and 3E). We did not see direct interactions between EDEM1, EDEM3 and SEL1L (Figure 3D). These observations lead us to propose a model for the increase in ERAD activity observed in UBC6e$^{-/-}$ cells. In wild-type cells, glycoproteins carrying G_1M_9 bind to CNX to await folding. However, in UBC6e$^{-/-}$ cells, the increase in EDEM1 and EDEM3 allows for prolonged interactions with CNX, as well as with the protein substrates bound to CNX. These interactions accelerate mannose trimming on CNX-bound substrates. The more extensively mannose-trimmed substrates no longer bind to CNX and are carried over to the HRD1-SEL1L ERAD complex through interaction with OS-9 (Figure 3F).

ER localization and the identity of its transmembrane domain are essential for UBC6e activity

UBC6e regulates the level of ERAD enhancers in order to attenuate ERAD. To assess the importance of proper localization of UBC6e and compare its function with that of mislocalized UBC6e, we generated a cytosolic variant of UBC6e by removal of its C-terminal tail anchor (ΔTM); a version in which the tail anchor is replaced with that of MAVS, a protein targeted to the mitochondria (Seth et al., 2005); and a variant with the transmembrane segment of the type I membrane protein CD4 (Figure 4A). The latter construct carries the transmembrane segment in opposite polarity to that of native CD4, yet inserts efficiently into the ER, as shown by glycosylation of an N-linked NXT/S acceptor sequence introduced into the predicted ER luminal portion (Claessen et al., 2010). Finally, we attached the E2 domain of UBC6e to the tail-anchor region of UBC6, the ER-localized and tail-anchored homolog of UBC6e (Figure S4A). Importantly, the E2 domains of all UBC6e mutants are exposed to the cytosol, as is the E2 domain of wild-type UBC6e. This allows an evaluation of the importance of cellular localization. We first confirmed that these variants localize to the respective intended compartments (Figure S3). Upon doxycycline-induced expression in UBC6e$^{-/-}$ cells, only wild-type UBC6e attenuated ERAD enhancers to

levels seen in wild-type cells (Figure 4B and S4E). We saw only partial down-regulation of ERAD enhancers by $UBC6e_{E2}$-$UBC6_{TM}$ and UBC6e-CD4, even when expressed at high levels (Figure 4B, S4B and S4E). In the absence of doxycycline, $UBC6e^{-/-}$ cells transduced with wild-type UBC6e still showed almost complete restoration of ERAD enhancer levels, presumably due to leaky promoter activity that allows for expression at about 10% of the wild-type level (data not shown).

We further investigated whether the transmembrane domain of UBC6e is important for its interaction with ERAD enhancers. Only UBC6e with its native transmembrane domain interacts with OS-9 and SEL1L, while interaction with EDEM1 cannot be detected by immunoprecipitation (Figure 4C, 4D, S4C and S4D). Even though wild-type UBC6e, UBC6e-CD4 and $UBC6e_{E2}$-$UBC6_{TM}$ all localize to the ER, UBC6e-CD4 and $UBC6e_{E2}$-$UBC6_{TM}$ down-regulate ERAD enhancers only partially, presumably because they were unable to stably interact with them.

Proper complex formation is essential for UBC6e function

We fractionated various MEF cell lysates on 10-60% linear sucrose density gradients to study complex formation of UBC6e with its partners. For wild-type UBC6e, ~60% of UBC6e is recovered as monomers and ~40% appears in larger complexes (fractions 6-8). However, we observed a different UBC6e distribution profile in UBC6e-CD4 cells, indicating the inability of UBC6e-CD4 to fully engage in proper complex formation (Figure 5A). This result is in line with the observation that UBC6e-CD4, despite being localized to the ER, does not down-regulate ERAD enhancers to the same extent as does wild-type UBC6e (Figure 4B and S4E).

When wild-type cell lysates are fractionated, we observe a signal corresponding to a larger complex (fraction 6-8) that contains UBC6e and ERAD enhancers (Figure 5B). This must be the complex that is essential for UBC6e's function in maintaining proper ERAD enhancer levels, since these are the only fractions that contain all members of the complex. We confirmed that UBC6e interacts with OS-9 and SEL1L in this complex, as well as the interaction between OS-9 and SEL1L in the same complex (Figure 5C).

The enzymatically inactive C91S mutant of UBC6e, when over-expressed, might displace wild-type UBC6e from the complex and inhibit normal UBC6e function. We transduced wild-type MEF cells with wild-type or the C91S mutant of UBC6e under the control of a doxycycline-inducible promoter and titrated the expression of UBC6e. As expected, when the C91S mutant was overexpressed to levels about 10-fold over the endogenous level, ERAD enhancers accumulated in a manner similar to that seen in $UBC6e^{-/-}$ cells (Figure 5D). Overexpression of the C91S mutant replaces active UBC6e in the complex and prevents degradation of its usual substrates. Overexpression of wild-type UBC6e does not further reduce the levels of ERAD enhancers.

Derlin2 interacts with UBC6e in the complex involved in the regulation of ERAD enhancers

Having found at least two multi-molecular complexes in which UBC6e participates, we considered the presence of yet other complexes. We generated $Derlin2^{-/-}$ mice and MEF cell lines (Dougan et al., 2011), and showed that not only ERAD enhancers but also UBC6e

itself was upregulated (Figure S5). Derlin2 might thus be part of the same or a similar complex. Immunoprecipitation using anti-Derlin2 antiserum confirmed its binding to UBC6e in a manner that depends on the identity of the transmembrane domain of UBC6e (Figure 5E). Derlin2 levels do not change in UBC6e$^{-/-}$ cells transduced with any of the UBC6e mutants, suggesting that it is not a substrate regulated by UBC6e, but is a member of a UBC6e complex (Figure 1B).

UBC6e exists in at least two different configurations: as an apparent monomer and as part of a complex. Only UBC6e that is part of such complexes controls the levels of ERAD enhancers (Figure 5F).

Overexpression of EDEM1 accelerates degradation of wild-type tyrosinase

UBC6e controls the amount of ERAD enhancers in order to attenuate ERAD activity under normal circumstances. Increased ERAD activity would not be considered harmful to the cell if only misfolded substrates were subject to accelerated degradation. However, how ER quality control sensors would distinguish between folding intermediates and unfolded proteins is not immediately apparent, because at some point in time both carry the same G_1Man_9 form of N-glycans. We hypothesized that an increase in ERAD activity could be harmful by eliminating proteins that fold comparatively slowly, before they have had the chance to attain their native fold.

To investigate this possibility, we chose tyrosinase as a substrate that folds comparatively slowly. Tyrosinase is a melanocyte-specific type I membrane glycoprotein that catalyzes the rate-limiting step in the production of melanin (Wang and Hebert, 2006). It folds slowly, with 6 N-glycosylation sites and 15 cysteine residues poised to make intramolecular disulfide bonds. Only one-third of tyrosinase attains its properly folded state and is then exported to melanocytes (Wang and Hebert, 2006). Furthermore, a single mutation, C89R or A206T, renders the protein unable to fold and results in a complete diversion to the ERAD pathway (Svedine et al., 2004; Toyofuku et al., 2001). To impose increased ERAD activity, we expressed EDEM1-HA together with wild-type tyrosinase or the C89R mutant fused to YFP in HEK293T cells. Both tyrosinase mutants showed decreased accumulation when co-expressed with EDEM1. The C89R mutant is more sensitive to increased EDEM1 levels, underscoring a role for EDEM1 in the recognition of misfolded glycoproteins (Figure 6A). EDEM1 interacted with all tyrosinase-YFP constructs, as did endogenous EDEM1 (Figure 6B and Figure S6A and S6B). Even in wild type cells, the EDEM1-mediated ERAD pathway removes a fraction of wild-type tyrosinase.

Increased degradation of tyrosinase in UBC6e$^{-/-}$ cells

UBC6e$^{-/-}$ cells have increased ERAD activity for two model ERAD substrates, NHK and RI332 (Figure 2B and 2C). Would ERAD also affect proteins known to fold comparatively slowly, such as wild-type tyrosinase? We observed less accumulation of tyrosinase-YFP in UBC6e$^{-/-}$ cells. This phenotype is reversed by expression of wild-type UBC6e but not the C91S mutant (Figure 6C). Similar to the canonical ERAD substrates, in pulse chase experiments, tyrosinase-YFP showed accelerated degradation in UBC6e$^{-/-}$ cells, most clearly during the lag phase ($t_{1/2}$ ~180 min in wild-type cells, $t_{1/2}$ ~90min in UBC6e$^{-/-}$ cells; Figure

6D). Inclusion of ZL_3VS stabilizes tyrosinase-YFP, indicating that degradation of tyrosinase is indeed proteasomal and mediated by the ERAD pathway (Figure 6D). The immunoprecipitated wild-type tyrosinase-YFP fusion showed strong interactions with EDEM1, EDEM3 and OS-9 in UBC6e$^{-/-}$ cells and UBC6e$^{-/-}$ cells transduced with C91S UBC6e (Figure 6E), consistent with the model proposed in Figure 3F.

We tracked maturation of tyrosinase by observing its acquisition of EndoH-resistance. Less endoH-resistant tyrosinase appeared in UBC6e$^{-/-}$ cells than in wild-type cells (Figure 6F and S6C). Addition of ZL_3VS increased the amount of EndoH-resistant tyrosinase in both cell lines, presumably by allowing more tyrosinase molecules the opportunity to attain an export-competent state (Figure S6C). Dislocation of misfolded proteins is kinetically coupled to their degradation, and therefore stalling proteasomal degradation is expected to lead to the accumulation of all intermediates upstream of the block, including those that have yet to leave the ER (Wiertz et al., 1996).

We quantified the fraction of EndoH-resistant tyrosinase for each chase timepoint (Figure 6F). There is a slight decrease in the fraction of EndoH-resistant tyrosinase in UBC6e$^{-/-}$ cells. While this trend is clear, the difference observed nonetheless fails to reach statistical significance. This difference is much smaller than the faster degradation rate observed (Figure 6D).

When analyzed under non-reducing conditions, tyrosinase-YFP from UBC6e$^{-/-}$ cells had a more diffuse appearance at the 4-hour time point (Figure S6D). To distinguish between differences in glycosylation versus redox state of tyrosinase as contributing factors, we analyzed samples with and without EndoH treatment, followed by separation by non-reducing SDS-PAGE (Figure S6E). Treatment with EndoH should remove glycan modifications on ER-resident tyrosinase. Any remaining differences in mobility might thus provide an indication of different redox states of tyrosinase. We observed similar redox states of tyrosinase in wild-type and UBC6e$^{-/-}$ MEFs (Figure S6E). Thus the more diffuse tyrosinase band in UBC6e$^{-/-}$ cells must result from differences in N-linked glycans. Deletion of UBC6e does not affect the redox state of tyrosinase but rather its N-glycan modifications, possibly through up-regulation of ERAD enhancers. Increased turnover concerns the pool of folding intermediates and is responsible for the reduction of the mature form of tyrosinase.

UBC6e$^{-/-}$ mice have reduced skin tyrosinase levels

ERAD activity in an UBC6e$^{-/-}$ environment affects not only artificial substrate degradation, but also the maturation of wild-type tyrosinase in MEFs, as shown above. To examine whether this finding applied also *in vivo*, we assessed the level of endogenous tyrosinase in the mouse epidermis, as this organ is the site of highest tyrosinase expression. We collected skin lysates from a wild-type mouse, a heterozygous UBC6e$^{+/-}$ mouse and two UBC6e$^{-/-}$ mice. Endogenous tyrosinase levels in UBC6e$^{-/-}$ mice are quite low as assessed by immunoblotting (Figure 7A). We therefore used skin lysates in a first round of immunoprecipitation to enrich for tyrosinase, followed by immunoblotting to detect the recovered tyrosinase. We observed a clear reduction in tyrosinase levels only in samples from UBC6e$^{-/-}$ mice (Figure 7B). The reduction in total tyrosinase levels correlate with our observations made in cell lines (Figure 6C) and correlated with the up-regulation of ERAD

enhancers in UBC6e$^{-/-}$ skin lysates. UBC6e$^{+/-}$ and wild-type samples showed comparable results, even with a significant reduction in UBC6e levels in the UBC6e$^{+/-}$ sample (Figure 7C).

Discussion

ER quality control serves to remove misfolded proteins and distinguishes between fully functional, folded proteins, which are spared from degradation, and terminally misfolded proteins, which are destroyed (Koenig and Ploegh, 2014; Smith et al., 2011). Only few cases are known in which an otherwise fully functional protein is degraded in the ER. A physiological example is the regulation of HMG-CoA-reductase (HMGR) by the intracellular levels of lanosterol. HMGR and lanosterol levels are inversely correlated, with excess HMGR being degraded by the ERAD pathway (Hampton and Garza, 2009). Pathogen-specific events can also control protein levels in the ER: the US2, US3 and US11 glycoproteins encoded by human cytomegalovirus (HCMV) co-opt the ERAD pathway to degrade Class I MHC heavy chains (Morito and Nagata, 2015). Our findings suggest a new layer of homeostatic control, in which ERAD activity itself is regulated by controlling the levels of select components through the action of UBC6e. The targets of this regulation are EDEM1, EDEM3, OS-9 and SEL1L (ERAD enhancers). Ablation of UBC6e causes up-regulation of active ERAD enhancers and so enhances clearance not only of terminally misfolded substrates but also of wild-type glycoproteins that fold comparatively slowly, such as tyrosinase.

ERAD enhancers are relatively short-lived proteins at steady state. Their mode of degradation and the molecular features that help explain their rather short half-life remained to be characterized. The present work on UBC6e provides insight into the underlying mechanisms. Deletion of UBC6e results in accumulation of ERAD enhancers without overt activation of the UPR (Figure 1B and 1E). This increase depends on the E2 enzymatic activity of UBC6e, its exact localization and on proper engagement in complex formation in its ER environment (Figure 1F, 4B and S4B). SEL1L is a possible candidate as the primary target for UBC6e-dependent degradation. However, UBC6e is an E2 ubiquitin-conjugating enzyme and E2s are not commonly considered to directly recognize their targets. The associated E3s, or the E2/E3 complexes are usually viewed as the elements responsible for substrate recognition. The identity of the E3 (or E3s) responsible for the observed down-regulation of EDEM1, OS-9 and Sel1L by UBC6e remains to be established.

Overexpression of catalytically inactive UBC6e in wild-type MEFs causes a dominant negative effect, whereas overexpression of wild-type UBC6e did not affect ERAD enhancer levels (Figure 5D). Deletion of UBC6e does not change EDEM2 levels (Figure 2F), suggesting that EDEM2 activity is presumably independent of ERAD activation. Careful regulation of the degradative capacity of these ERAD factors therefore operates at steady state in the absence of obvious stressors. When we replaced the C-terminal segment of UBC6e with that of the integral membrane protein CD4 or that of the tail-anchored protein UBC6, these chimeras were less active in normalizing ERAD enhancer levels in UBC6e$^{-/-}$ cells (Figure 4B and S4B). The CD4 and UBC6 chimeras did not interact with OS-9 or SEL1L (Figure 4C, 4D, S4C and S4D). The activity of such UBC6e complexes, which help

establish the ERAD capacity of the ER, may thus have been compromised, Even expression at ~10% of the endogenous level of UBC6e in UBC6e$^{-/-}$ cells re-establishes ERAD enhancer levels to those seen in wild-type cells: apparently very little UBC6e suffices to properly regulate them. Knock-down of UBC6e by means of siRNA delayed degradation of CFTRΔF508 and Class I MHC heavy chains (Burr et al., 2011; Younger et al., 2006). Knock-down mediated by siRNA or shRNA is rarely complete, yet may have been sufficient to examine the role of UBC6e in canonical ERAD, but would not have achieved the reduction required to observe control of ERAD enhancer levels by UBC6e. UBC6e$^{-/-}$ cells up-regulate selective ERAD-related factors with a concomitant increase in ERAD activity. The HRD1 ERAD complex may accept multiple E2s for degradation of terminally misfolded substrates, whereas degradation of folding-competent ERAD enhancers apparently requires only UBC6e as the functional E2 responsible.

Even if the ER engages in normal rates of cell type-appropriate protein synthesis and if overloading with misfolded proteins can be avoided, mechanisms of quality control should still apply at steady state and under normal conditions of growth, because errors in protein synthesis and protein folding cannot be avoided completely. Dysregulated ERAD activity as the result of deletion of key ERAD components such as HRD1 or SEL1L showed embryonic lethality in mice (Sun et al., 2014; Yagishita et al., 2005). MEFs deficient in HRD1 or SEL1L tend to accumulate canonical ERAD substrates and show activation of the UPR (Kaneko et al., 2010). In contradistinction, exaggerated ERAD activity may lead to loss-of-function through premature degradation of potentially functional proteins that have yet to attain their final and stable conformation (Noack et al., 2014). It has been difficult to test this notion experimentally due to the inability to initiate a more active ERAD pathway in the absence of triggering the UPR. The precise sequence of steps that control the mammalian ERAD pathway remains to be established and further adds to the challenge.

Here we addressed this question by exploring the mechanism of increased ERAD activity mediated by increased levels of ERAD components, as brought about by the ablation of UBC6e (Figure 7E). Our observations support the ‘mannose timer hypothesis’ (Fagioli, 2001; Helenius et al., 1997). In the course of the CNX/CRT cycle, terminally misfolded substrates are not distinguishable by any presently known criterion from folding intermediates, since both can carry the same G_1Man_9 N-glycan(s). EDEM2 and the other EDEM family proteins are functionally distinct, as inferred from cells that lack EDEM2 (Ninagawa et al., 2014). Glycoproteins whose N-linked glycans showed advanced mannose trimming could no longer attain their native structure, and were targeted for degradation. They could no longer productively engage the CNX/CRT cycle, nor could they serve as substrates for the folding sensor UGGT. Up-regulation of OS-9 and SEL1L facilitates the transfer of ERAD substrates from CNX to the HRD1-centered ERAD machinery and so enhances overall ERAD activity. We have shown that ERAD of glycoproteins is indeed regulated in a UBC6e-dependent manner. The non-glycoprotein ERAD pathway is far less well understood, presumably differs from the pathway we explored here and merits a separate and detailed analysis.

Under normal conditions and in the absence of obvious stressors, ERAD also promotes the degradation of proteins that fold comparatively slowly, such as proteins with many disulfide

bonds and/or with many transmembrane segments (Guerriero and Brodsky, 2012). The folding intermediates of proteins that fall into these categories require prolonged engagement of the CNX/CRT cycle to allow completion of correct folding. We hypothesized that the increases in ERAD activity seen upon ablation of UBC6e might interfere with normal maturation of these slow-folding proteins and would thus compromise their function by reducing their levels. Indeed, tyrosinase showed accelerated degradation and failed to mature in both UBC6e$^{-/-}$ cells in tissue culture and in the skin of mice. Deletion of UBC6e does not affect the overall secretion of glycoproteins as assayed in vitro (Figure 7D and S7). Therefore, deletion of UBC6e showed only a minor effect in mice, compared with the ablation of other key ERAD components.

Transcription is usually considered the main contributor to the regulation of the ER quality control machinery. Regulation of ER homeostasis under the agency of ATF6, PERK and Ire1α in the course of the unfolded protein response (UPR) are well-established examples (Hetz et al., 2015), the manipulation of which usually requires the use of chemical stressors such as thapsigargin, tunicamycin or DTT. How the activity of ERAD is controlled at steady state and in the absence of any ER stressors therefore remains an important question. We show that ERAD accelerators are members subject to quantity control in the ER by a UBC6e-dependent degradation pathway. The male sterility and auditory defects seen in UBC6e$^{-/-}$ mice might result from premature degradation of slow-folding proteins that participate in these processes. Post-transcriptional control of the ERAD machinery uncovered here is yet another means of homeostatic ER quality control.

Experimental Procedures

Plasmids, Antibodies, and Reagents

Plasmids, antibodies, and reagents are described in the Supplemental Experimental Procedures.

Cell Culture and Transfection

Cells were grown in Dulbecco's modified Eagle's medium (DMEM) supplemented with 10% inactivated fetal bovine serum with or without 0.0007% v/v β-mercaptoethanol. Transient transfections were performed using Lipofectamine 2000 for HEK293T cells, Lipofectamine 3000 for MEFs according to the manufacturer's instructions (Invitrogen). Further experiments were performed 24 h after transfection.

Lentiviral Infection

Lentiviruses were generated in HEK293T cells. MEFs stably expressing various UBC6e mutants were created by lentiviral infection, followed by selection with geneticin or puromycin. See the Supplemental Experimental Procedures for details.

Mouse Experiments

All mouse experiments were performed in compliance with the protocols approved by the Massachusetts Institute of Technology Committee on Animal Care.

Fluorescence Microscopy

Images captured by confocal microscopes were viewed and processed by a PerkinElmer confocal system and Velocity software. Images were captured using a confocal microscope with a 63°- 1.40 N.A. of the Carl Zeiss Plan Apo oil objective. See the Supplemental Experimental Procedures for detail.

Immunoprecipitation and Western Blot

Cells were lysed in lysis buffer and subjected to immunoprecipitations with primary antibody. Immuno complexes were subjected to SDS-PAGE and analyzed by immunoblot. For details of detergents, conditions and antibodies used, see the Supplemental Experimental Procedures.

Pulse-Chase Analysis and Glucosidase Digestions

For pulse-labeling experiments, cells were starved for 45–60 min in methionine/cysteine-free DMEM at 37 °C, and labeled for 15-30 min at a concentration of 0.1mCi/ml of [^{35}S] methionine/cysteine, followed by incubation in complete MEF medium during the chase periods. Cell lysates were subjected to immunoprecipitation, followed by SDS-PAGE and examined by fluorography analysis. An EndoH digestion of radiolabeled substrates was performed after immunoprecipitation according to the manufacturer's instructions (New England Biolabs). See the Supplemental Experimental Procedures for details.

Sucrose Density Gradient Fractionation

Post-nuclear supernatants were applied to a 10%-60% linear sucrose gradient and centrifuged at 160,000 g for 16 hr. Fractions were collected from the top and used for further analysis.

Statistical Analysis

Welch's t-test was used for statistical analysis. P value less than 0.05 were considered statistically significant.

Supplementary Material

Refer to Web version on PubMed Central for supplementary material.

Acknowledgments

We thank members of the Ploegh laboratory, especially F. Schmidt, R. Cheloha and M. Truttmann, for critical reading of the manuscript. We thank Tom DiCesare for illustrations, Wendy Salmon of the Keck facility at the Whitehead Institute for imaging. This work was supported by the National Institutes of Health to H.L.P, Japan Society for the Promotion of Science to M.H., the Uehara Memorial Foundation to M.H, and ASTAR NSS (PhD) scholarship to J.L.

References

Burr ML, Cano F, Svobodova S, Boyle LH, Boname JM, Lehner PJ. HRD1 and UBE2J1 target misfolded MHC class I heavy chains for endoplasmic reticulum-associated degradation. Proc Natl Acad Sci U S A. 2011; 108:2034–2039. [PubMed: 21245296]

Christianson JC, Shaler TA, Tyler RE, Kopito RR. OS-9 and GRP94 deliver mutant α1-antitrypsin to the Hrd1-SEL1L ubiquitin ligase complex for ERAD. Nat Cell Biol. 2008; 10:272–282. [PubMed: 18264092]

Claessen JHL, Mueller B, Spooner E, Pivorunas VL, Ploegh HL. The transmembrane segment of a tail-anchored protein determines its degradative fate through dislocation from the endoplasmic reticulum. J Biol Chem. 2010; 285:20732–20739. [PubMed: 20435896]

Cormier JH, Tamura T, Sunryd JC, Hebert DN. EDEM1 Recognition and Delivery of Misfolded Proteins to the SEL1L-Containing ERAD Complex. Mol Cell. 2009; 34:627–633. [PubMed: 19524542]

Dougan SK, Hu CCA, Paquet ME, Greenblatt MB, Kim J, Lilley BN, Watson N, Ploegh HL. Derlin-2-deficient mice reveal an essential role for protein dislocation in chondrocytes. Mol Cell Biol. 2011; 31:1145–1159. [PubMed: 21220515]

Ellgaard L, Frickel EM. Calnexin, calreticulin, and ERp57: teammates in glycoprotein folding. Cell Biochem Biophys. 2003; 39:223–247. [PubMed: 14716078]

Fagioli C. Glycoprotein Quality Control in the Endoplasmic Reticulum. Mannose trimming by endoplasmic reticulum mannosidase i times the proteasomal degradation of unassembled immunoglobulin subunits. J Biol Chem. 2001; 276:12885–12892. [PubMed: 11278527]

Guerriero CJ, Brodsky JL. The Delicate Balance Between Secreted Protein Folding and Endoplasmic Reticulum-Associated Degradation in Human Physiology. Physiol Rev. 2012; 92:537–576. [PubMed: 22535891]

Hampton RY, Garza RM. Protein Quality Control as a Strategy for Cellular Regulation: Lessons from Ubiquitin-Mediated Regulation of the Sterol Pathway. Chem Rev. 2009; 109:1561–1574. [PubMed: 19243134]

Helenius, a; Trombetta, ES.; Hebert, DN.; Simons, JF. Calnexin, calreticulin and the folding of glycoproteins. Trends Cell Biol. 1997; 7:193–200. [PubMed: 17708944]

Hetz C, Chevet E, Oakes SA. Proteostasis control by the unfolded protein response. Nat Cell Biol. 2015; 17:829–838. [PubMed: 26123108]

Hirao K, Natsuka Y, Tamura T, Wada I, Morito D, Natsuka S, Romero P, Sleno B, Tremblay LO, Herscovics A, et al. EDEM3, a soluble EDEM homolog, enhances glycoprotein endoplasmic reticulum-associated degradation and mannose trimming. J Biol Chem. 2006; 281:9650–9658. [PubMed: 16431915]

Hosokawa N, Wada I, Hasegawa K, Yorihuzi T, Tremblay LO, Herscovics a, Nagata K. A novel ER alpha-mannosidase-like protein accelerates ER-associated degradation. EMBO Rep. 2001; 2:415–422. [PubMed: 11375934]

Iida Y, Fujimori T, Okawa K, Nagata K, Wada I, Hosokawa N. SEL1L Protein Critically Determines the Stability of the HRD1-SEL1L Endoplasmic Reticulum-associated Degradation (ERAD) Complex to Optimize the Degradation Kinetics of ERAD Substrates. J Biol Chem. 2011; 286:16929–16939. [PubMed: 21454652]

Kaneko M, Koike H, Saito R, Kitamura Y, Okuma Y, Nomura Y. Loss of HRD1-Mediated Protein Degradation Causes Amyloid Precursor Protein Accumulation and Amyloid- Generation. J Neurosci. 2010; 30:3924–3932. [PubMed: 20237263]

Koenig PA, Ploegh HL. Protein quality control in the endoplasmic reticulum. F1000Prime Rep. 2014

Koenig PA, Nicholls PK, Schmidt FI, Hagiwara M, Maruyama T, Frydman GH, Watson N, Page DC, Ploegh HL. The E2 Ubiquitin-conjugating Enzyme UBE2J1 Is Required for Spermiogenesis in Mice. J Biol Chem. 2014; 289:34490–34502. [PubMed: 25320092]

Lenk U, Yu H, Walter J, Gelman MS, Hartmann E, Kopito RR, Sommer T. A role for mammalian Ubc6 homologues in ER-associated protein degradation. Journal of Cell Science. 2002; 115:3007–3014. [PubMed: 12082160]

Menon MB, Tiedje C, Lafera J, Ronkina N, Konen T, Kotlyarov A, Gaestel M. Endoplasmic reticulum-associated ubiquitin-conjugating enzyme Ube2j1 is a novel substrate of MK2 (MAPKAP kinase-2) involved in MK2-mediated TNFα production. Biochem J. 2013; 456:163–172. [PubMed: 24020373]

Molinari M. Role of EDEM in the Release of Misfolded Glycoproteins from the Calnexin Cycle. Science (80-). 2003; 299:1397–1400.

Morito D, Nagata K. Pathogenic Hijacking of ER-Associated Degradation: Is ERAD Flexible? Mol Cell. 2015; 59:335–344. [PubMed: 26253026]

Mueller B, Lilley BN, Ploegh HL. SEL1L, the homologue of yeast Hrd3p, is involved in protein dislocation from the mammalian ER. J Cell Biol. 2006; 175:261–270. [PubMed: 17043138]

Mueller B, Klemm EJ, Spooner E, Claessen JH, Ploegh HL. SEL1L nucleates a protein complex required for dislocation of misfolded glycoproteins. Proc Natl Acad Sci U S A. 2008; 105:12325–12330. [PubMed: 18711132]

Ninagawa S, Okada T, Sumitomo Y, Kamiya Y, Kato K, Horimoto S, Ishikawa T, Takeda S, Sakuma T, Yamamoto T, et al. EDEM2 initiates mammalian glycoprotein ERAD by catalyzing the first mannose trimming step. J Cell Biol. 2014; 206:347–356. [PubMed: 25092655]

Noack J, Bernasconi R, Molinari M. How Viruses Hijack the ERAD Tuning Machinery. J Virol. 2014; 88:10272–10275. [PubMed: 24990995]

Oda Y. EDEM As an Acceptor of Terminally Misfolded Glycoproteins Released from Calnexin. Science (80-). 2003; 299:1394–1397.

Olivari S, Galli C, Alanen H, Ruddock L, Molinari M. A novel stress-induced EDEM Variant regulating endoplasmic reticulum-associated glycoprotein degradation. J Biol Chem. 2005; 280:2424–2428. [PubMed: 15579471]

Palade G. Intracellular aspects of the process of protein synthesis. Science. 1975; 189:867. [PubMed: 17812524]

Reggiori F, Monastyrska I, Verheije MH, Calì T, Ulasli M, Bianchi S, Bernasconi R, de Haan CaM, Molinari M. Coronaviruses Hijack the LC3-I-positive EDEMosomes, ER-derived vesicles exporting short-lived ERAD regulators, for replication. Cell Host Microbe. 2010; 7:500–508. [PubMed: 20542253]

Satoh T, Chen Y, Hu D, Hanashima S, Yamamoto K, Yamaguchi Y. Structural Basis for Oligosaccharide Recognition of Misfolded Glycoproteins by OS-9 in ER-Associated Degradation. Mol Cell. 2010; 40:905–916. [PubMed: 21172656]

Seth RB, Sun L, Ea CK, Chen ZJ. Identification and Characterization of MAVS, a Mitochondrial Antiviral Signaling Protein that Activates NF-κB and IRF3. Cell. 2005; 122:669–682. [PubMed: 16125763]

Sifers RN, Brashears-Macatee S, Kidd VJ, Muensch H, Woo SLC. A frameshift mutation results in a truncated α1-antitrypsin that is retained within the rough endoplasmic reticulum. J Biol Chem. 1988; 263:7330–7335. [PubMed: 3259232]

Smith MH, Ploegh HL, Weissman JS. Road to Ruin: Targeting Proteins for Degradation in the Endoplasmic Reticulum. Science (80-). 2011; 334:1086–1090.

Stein A, Ruggiano A, Carvalho P, Rapoport Tom A. Key Steps in ERAD of Luminal ER Proteins Reconstituted with Purified Components. Cell. 2014; 158:1375–1388. [PubMed: 25215493]

Sun S, Shi G, Han X, Francisco AB, Ji Y, Mendonça N, Liu X, Locasale JW, Simpson KW, Duhamel GE, et al. Sel1L is indispensable for mammalian endoplasmic reticulum-associated degradation, endoplasmic reticulum homeostasis, and survival. Proc Natl Acad Sci U S A. 2014; 111:E582–E591. [PubMed: 24453213]

Svedine S, Wang T, Halaban R, Hebert DN. Carbohydrates act as sorting determinants in ER-associated degradation of tyrosinase. J Cell Sci. 2004; 117:2937–2949. [PubMed: 15161941]

Toyofuku K, Wada I, Spritz Ra, Hearing VJ. The molecular basis of oculocutaneous albinism type 1 (OCA1): sorting failure and degradation of mutant tyrosinases results in a lack of pigmentation. Biochem J. 2001; 355:259–269. [PubMed: 11284711]

Tsao YS, Ivessa NE, Adesnik M, Sabatini DD, Kreibich G. Carboxy terminally truncated forms of ribophorin I are degraded in pre-Golgi compartments by a calcium-dependent process. J Cell Biol. 1992; 116:57–67. [PubMed: 1730749]

Wang N, Hebert DN. Tyrosinase maturation through the mammalian secretory pathway: Bringing color to life. Pigment Cell Res. 2006; 19:3–18. [PubMed: 16420243]

Wiertz EJHJ, Jones TR, Sun L, Bogyo M, Geuze HJ, Ploegh HL. The human cytomegalovirus US11 gene product dislocates MHC class I heavy chains from the endoplasmic reticulum to the cytosol. Cell. 1996; 84:769–779. [PubMed: 8625414]

van Wijk SJL, Timmers HTM. The family of ubiquitin-conjugating enzymes (E2s): deciding between life and death of proteins. FASEB J. 2010; 24:981–993. [PubMed: 19940261]

Xu C, Ng DTW. Glycosylation-directed quality control of protein folding. Nat Rev Mol Cell Biol. 2015 needs page numbers etc.

Yagishita N, Ohneda K, Amano T, Yamasaki S, Sugiura A, Tsuchimochi K, Shin H, Kawahara Ki, Ohneda O, Ohta T, et al. Essential Role of Synoviolin in Embryogenesis. J Biol Chem. 2005; 280:7909–7916. [PubMed: 15611074]

Yoshida H, Matsui T, Hosokawa N, Kaufman RJ, Nagata K, Mori K. A time-dependent phase shift in the mammalian unfolded protein response. Dev Cell. 2003; 4:265–271. [PubMed: 12586069]

Younger JM, Chen L, Ren HY, Rosser MFN, Turnbull EL, Fan CY, Patterson C, Cyr DM. Sequential Quality-Control Checkpoints Triage Misfolded Cystic Fibrosis Transmembrane Conductance Regulator. Cell. 2006; 126:571–582. [PubMed: 16901789]

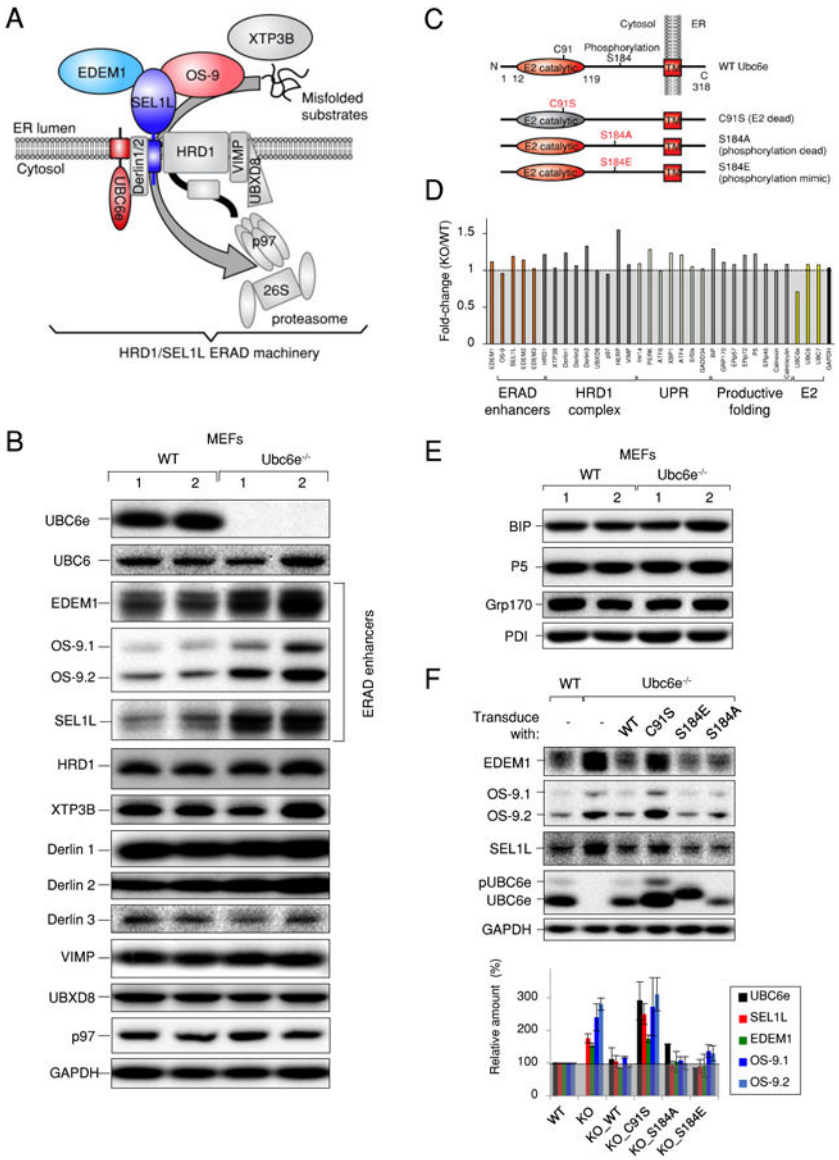

Figure 1. Selective ERAD components are regulated by UBC6e

(A) Model showing the components in the canonical HRD1-containing ERAD complex.

(B) ERAD enhancers are selectively up-regulated in two independently derived UBC6e$^{-/-}$ lines of MEFs.

(C) No significant difference is observed for mRNA levels of ER quality control-related genes in wild-type and UBC6e$^{-/-}$ cells. Quantifications of the mRNA expression ratio (KO/WT) of ER-resident E2s and the genes related to ERAD, UPR, productive folding are shown.

(D) Levels of the UPR target proteins BiP, P5 and Grp170 do not differ in wild-type and UBC6e$^{-/-}$ cells.

(E) Scheme for UBC6e structure and the mutants used. Mutation in the active site residue C91 renders the protein enzymatically inactive (Lenk et al., 2002). Phosphorylation occurs at S184 (Menon et al., 2013).

(F) Up-regulation of ERAD enhancers in UBC6e$^{-/-}$ MEF cells is reversed by re-introduction of catalytically active versions of UBC6e. UBC6e$^{-/-}$ cells were transduced with UBC6e variants using pCDH-EF1-CMV-puro vector. Quantifications are normalized to GAPDH. Error bars represent S.D. (n=3). Phosphorylated UBC6e is referred to as pUBC6e.
See also Figure S1.

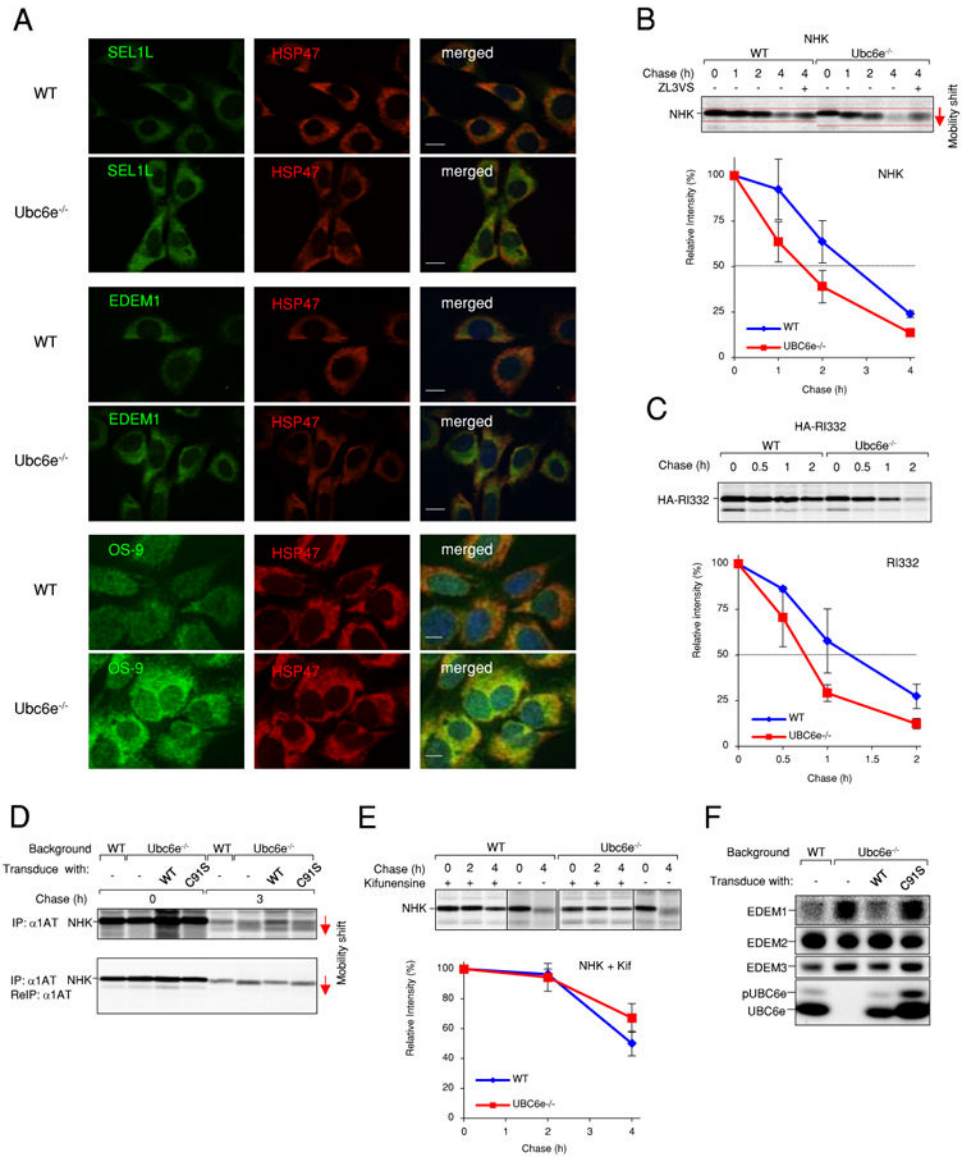

Figure 2. UBC6e deletion causes hyperactive ERAD for glycoprotein substrates

(A) Immunofluorescence of endogenous EDEM1, OS-9 and SEL1L in wild-type and UBC6e$^{-/-}$ cells. Cells are stained with anti-HSP47 as an ER marker.

(B) ERAD is enhanced for the Null Hong Kong (NHK) variant of α1-antitripsin in UBC6e$^{-/-}$ cells. Wild-type and UBC6e$^{-/-}$ cells were transfected with a NHK construct for 24 hours. The cells were starved for 1 hour, labeled with ^{35}S-Met/Cys for 20 min and chased for various time periods. Cells were treated with or without proteasome inhibitor ZL_3VS during the 4 hour chase period. NHK was immunoprecipitated using an α1-antitripsin antibody. Quantifications are normalized to t=0hr. Error bars represent S.D. (n=3).

(C) The glycoprotein ERAD substrate RI332 is degraded more rapidly in UBC6e$^{-/-}$ cells. Wild-type and UBC6e$^{-/-}$ MEFs were transfected with RI332-HA, pulsed for 15 minutes and chased for the indicated time periods. Cell lysates were immunoprecipitated using an anti-HA antibody. Quantifications are normalized to t=0hr. Error bars represent S.D. (n=3).

(D) NHK is deglycosylated more rapidly in cells that lack catalytically active UBC6e. Wild-type, UBC6e$^{-/-}$, and UBC6e$^{-/-}$ MEFs stably expressing wild-type or C91S UBC6e were transfected with NHK. Transfected cells were pulsed for 15 min and chased for 3 hours. NHK was either immunoprecipitated once (upper panel) or re-immunoprecipitated (lower panel) using an α1-antitrypsin antibody.

(E) Kifunensine treatment inhibits the mannose trimming-dependent mobility shift and the degradation of NHK in both wild-type and UBC6e$^{-/-}$ Cells. A pulse-chase experiment as shown in Figure 2B was performed with or without kifunensine treatment. Quantifications are normalized to t=0hr. Error bars represent S.D. (n=3)

(F) EDEM1 and EDEM3, but not EDEM2, are up-regulated in UBC6e-deficient cells.

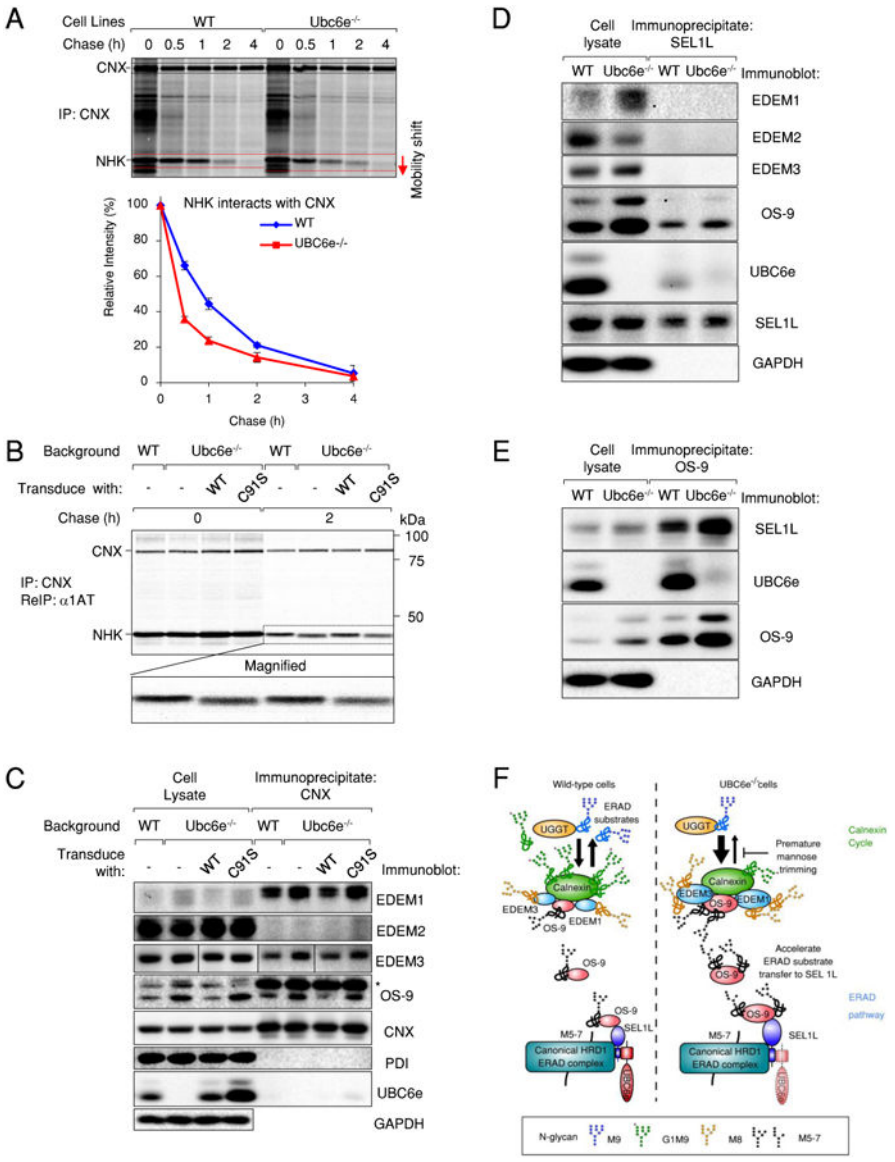

Figure 3. Deletion of UBC6e leads to pre-mature release of NHK from calnexin (CNX) and enhances interaction of ERAD enhancers

(G) (A) UBC6e deletion promotes the release of NHK from CNX. Wild-type and UBC6e$^{-/-}$ cells were transfected with NHK for 24 hours. Cells were starved for 1 hour, labeled with ^{35}S-Met/Cys for 20 min and chased for various time periods. Lysates were immunoprecipitated with an antibody to CNX. For quantification, the amount of labeled NHK was normalized relative to CNX for each sample. Error bars represent S.D. (n=3)

(B) NHK bound to CNX is deglycosylated in cells that lack functional UBC6e. Wild-type, UBC6e$^{-/-}$, and UBC6e$^{-/-}$ MEFs stably expressing wild-type or C91S UBC6e were transfected with NHK. Transfected cells were labeled for 20 mins and chased for 2 hours. The lysates were immunoprecipitated with a CNX antibody and re-immunoprecipitated using an α1-antitripsin antibody.

(C) More EDEM1, EDEM3 and OS-9 interact with CNX in UBC6e$^{-/-}$ cells. EDEM2 does not co-immunoprecipitate with CNX in either wild-type or UBC6e$^{-/-}$ cells.

(D-E) The amount of interacting SEL1L and OS-9 increases in UBC6e$^{-/-}$ cells. Co-immunoprecipitation of SEL1L and EDEM family proteins is not observed in either wild-type or UBC6e$^{-/-}$ cells.

(G) Model showing the comparison between wild-type and UBC6e$^{-/-}$ cells for a sequential pathway that moves ERAD substrates from productive folding in the CNX cycle to ERAD machineries.

See also Figure S2.

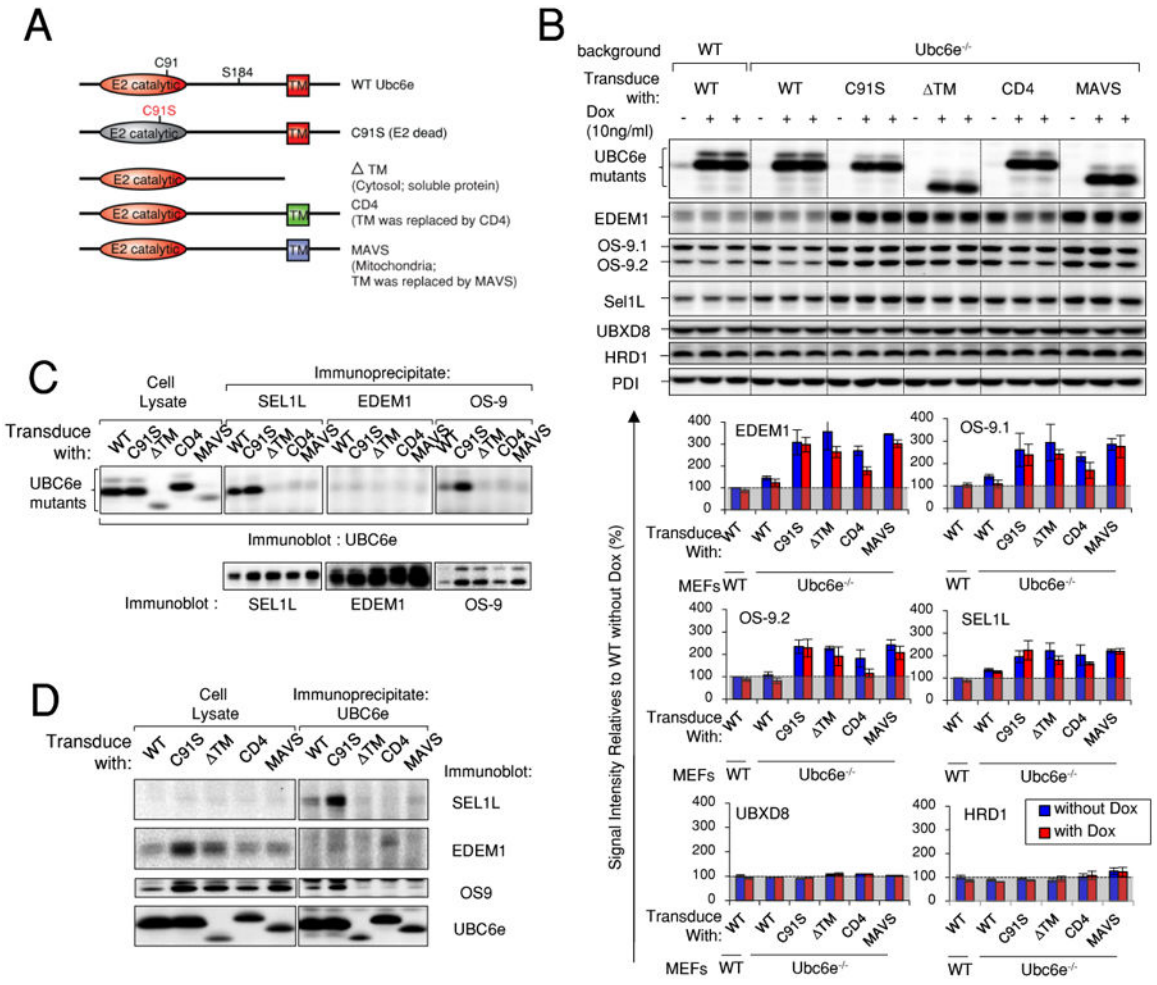

Figure 4. Precise ER membrane localization is important for UBC6e function and interaction with ERAD enhancers

(A) Scheme of the different transmembrane domain (TMD) mutants of UBC6e.

(B) Correct ER localization is essential for the function of UBC6e. Expression of UBC6e-TM mutants was induced using doxycycline for 24 hours. Only UBC6e$^{-/-}$ cells transduced with wild-type UBC6e showed down-regulation of ERAD enhancers to the extent seen in wild-type cells. The other ERAD components, UBXD8 and HRD1, were not affected. Quantification is normalized relative to PDI. Error bars represent S.D. (n=3)

(C-D) The correct transmembrane domain is necessary for UBC6e to interact with the substrates SEL1L and OS-9. UBC6e$^{-/-}$ cells expressing different UBC6e variants were collected in 2% CHAPS and immunoprecipitated with either antibodies against the EDEM1, OS-9 or SEL1L (C) or rabbit anti-UBC6e (D). Interactions between UBC6e and OS-9 or SEL1L were observed only in cells expressing wild-type or C91S UBC6e. We failed to observe interaction between UBC6e and EDEM1.

See also Figure S3 and S4.

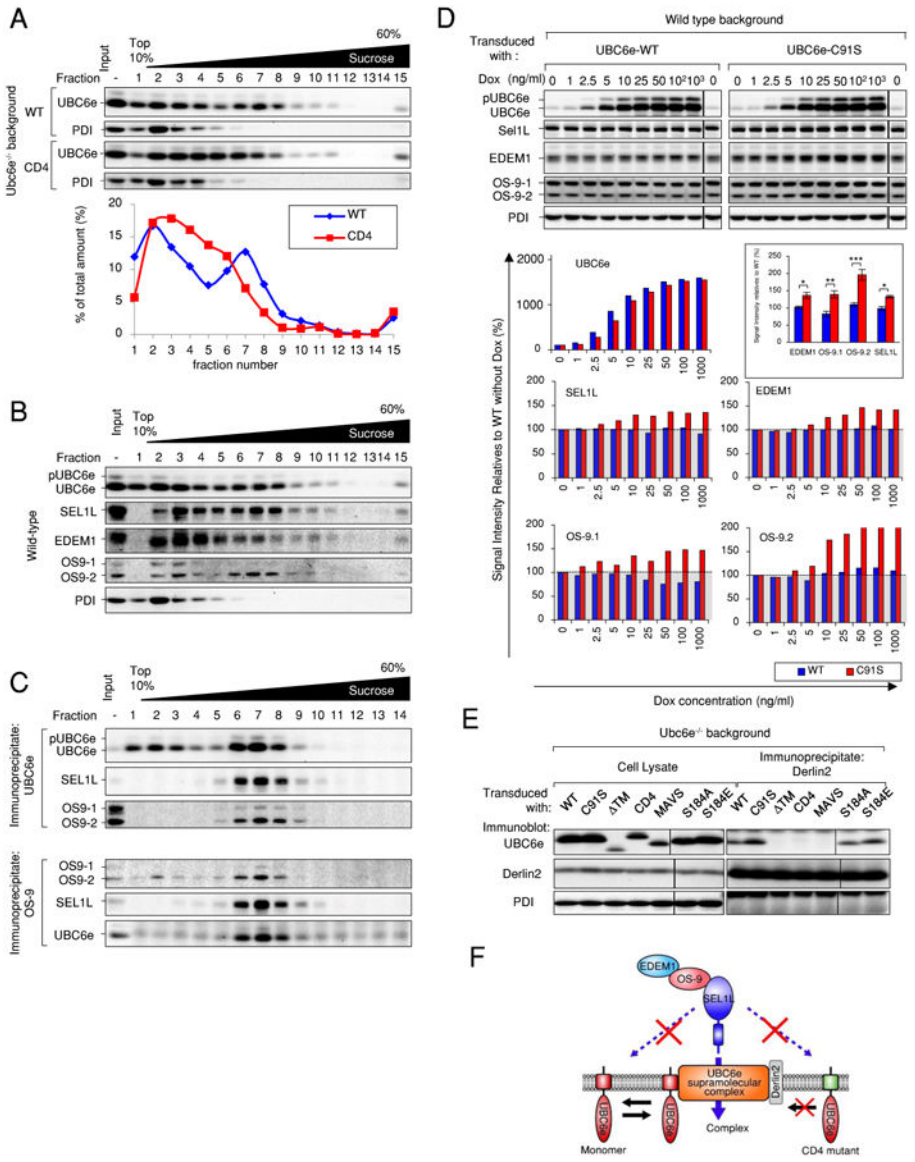

Figure 5. Participation in complex formation is essential for the function of UBC6e

(A) Wild-type UBC6e and UBC6e-CD4 fractionate differently in a sucrose density gradient. UBC6e$^{-/-}$ cells transduced with wild-type UBC6e and UBC6e-CD4 were lysed in 2% CHAPS and fractionated by centrifugation on a 10-60% linear sucrose gradient in the absence of detergent.

(B) UBC6e and its substrates exist both in monomeric form and in fractions that contain larger complexes.

(C) UBC6e interacts with its substrates only in fractions containing large complexes. Lysate fractions in (B) are immunoprecipitated with anti-UBC6e or anti-OS-9 followed by immunoblot with anti-UBC6e, anti-OS-9 or anti-SEL1L sera.

(D) UBC6e C91S acts as a dominant negative mutant that competes with wild-type UBC6e for complex formation and antagonizes UBC6e regulation of ERAD enhancers. Wild-type MEF cells were transduced with wild-type or C91S UBC6e using doxycycline-inducible

pINDUCER20 system and titrated for UBC6e expression. Statistical analysis was conducted on cells that reach induction saturation for UBC6e (>10 fold compared to endogenous). Statistical analysis is presented in the inset as means ± SEM, n = 8. *p < 0.05, **p < 0.001, ***p < 0.0001

(E) The UBC6e transmembrane domain is essential for its interaction with Derlin2. Cells were induced for 24 hours and lysed in 2% CHAPS, immunoprecipitated with anti-Derlin2 and blotted for the interaction with UBC6e.

(F) Model diagram showing that only UBC6e involved in complex are able to regulate SEL1L, OS-9 and EDEM1.

See also Figure S5.

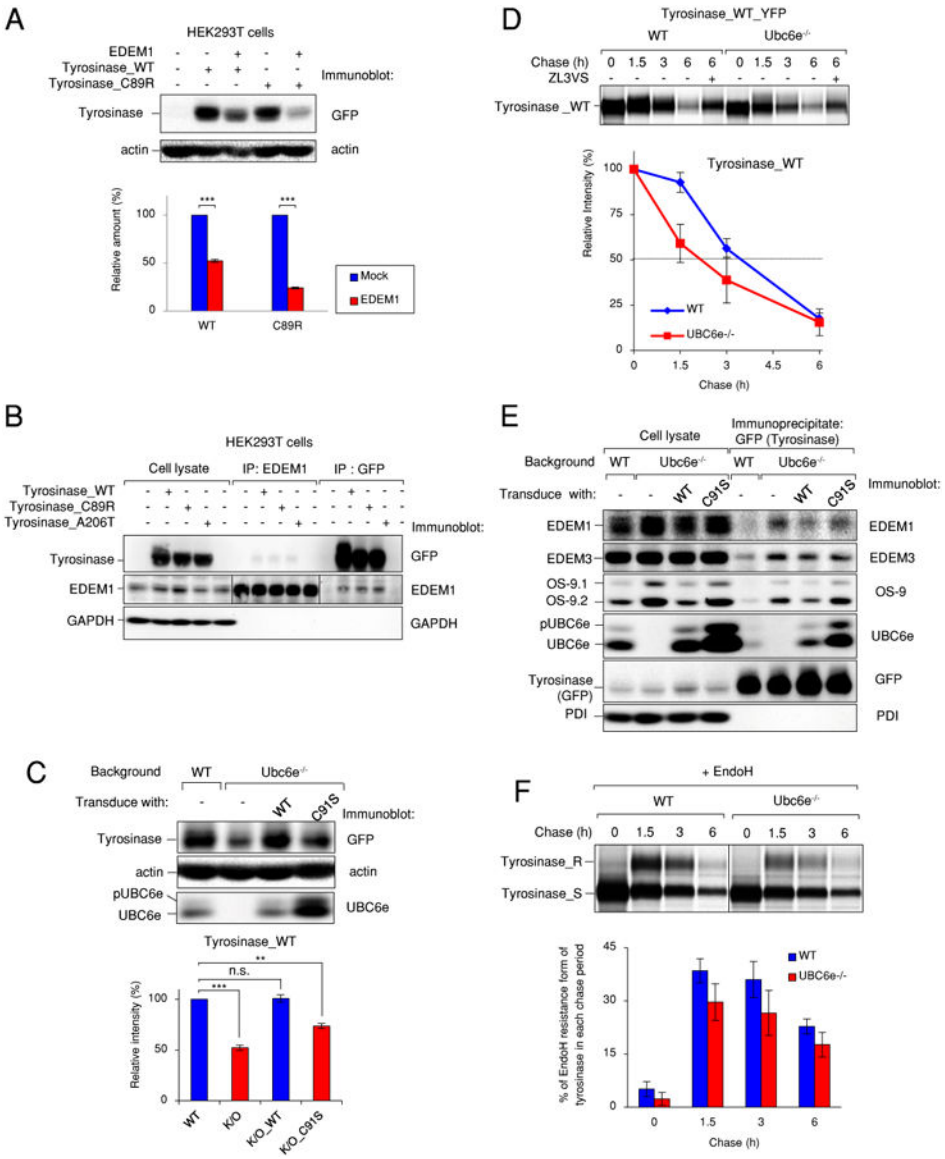

Figure 6. Hyperactive ERAD in UBC6e$^{-/-}$ cells accelerates degradation of the slow-folding substrate tyrosinase and inhibits maturation of tyrosinase

(A) Overexpression of EDEM1 accelerates degradation of both wild-type tyrosinase and C89R mutant. HEK293T cells were transfected with plasmids encoding EDEM1-HA and tyrosinase-YFP for 24 hours. The cells were lysed and immunoblotted for accumulation of tyrosinase-YFP. Error bars represent S.D. (n=3)

(B) Wild-type and mutant tyrosinases interact with endogenous EDEM1. HEK293T cells were transfected with wild-type, C89R or A206T tyrosinase-YFP fusion. Cells were lysed and immunoprecipitation with anti-GFP or anti-EDEM1.

(C) Wild-type tyrosinase accumulates less in cells that lack functional UBC6e. Wild-type, UBC6e$^{-/-}$ and UBC6e$^{-/-}$ stably expressing wild-type or C91S UBC6e are transfected with tyrosinase-YFP for 24 hours and analyzed for tyrosinase accumulation. Error bars represent S.D. (n=3)

(D) Degradation of wild-type tyrosinase is accelerated in UBC6e$^{-/-}$ MEFs. Cells transfected with tyrosinase-YFP were pulsed for 30 min with ^{35}S-Met/Cys and chased for the indicated periods. Cell lysates were immunoprecipitated with anti-GFP. ZL_3VS treatment blocks degradation of the fusion protein. Quantifications are normalized to t=0hr. Error bars represent S.D. (n=3)

(E) More EDEM1, EDEM3 and OS-9 co-immunoprecipitated with transfected tyrosinase-YFP in UBC6e$^{-/-}$ cells.

(F) Tyrosinase maturation and export to the post-ER compartments is inhibited by deletion of UBC6e. Cells were treated as in (D) and tyrosinase-YFP was immunoprecipitated with anti-GFP. The recovered samples were treated with Endoglycosidase H (EndoH). The fraction of EndoH-resistant tyrosinase-YFP in each chase time point was quantified. Error bars represent S.D. (n=3).

The statistical results are presented as means ± SEM, n = 4. **$p < 0.001$

***$p < 0.0001$

See also Figure S6.

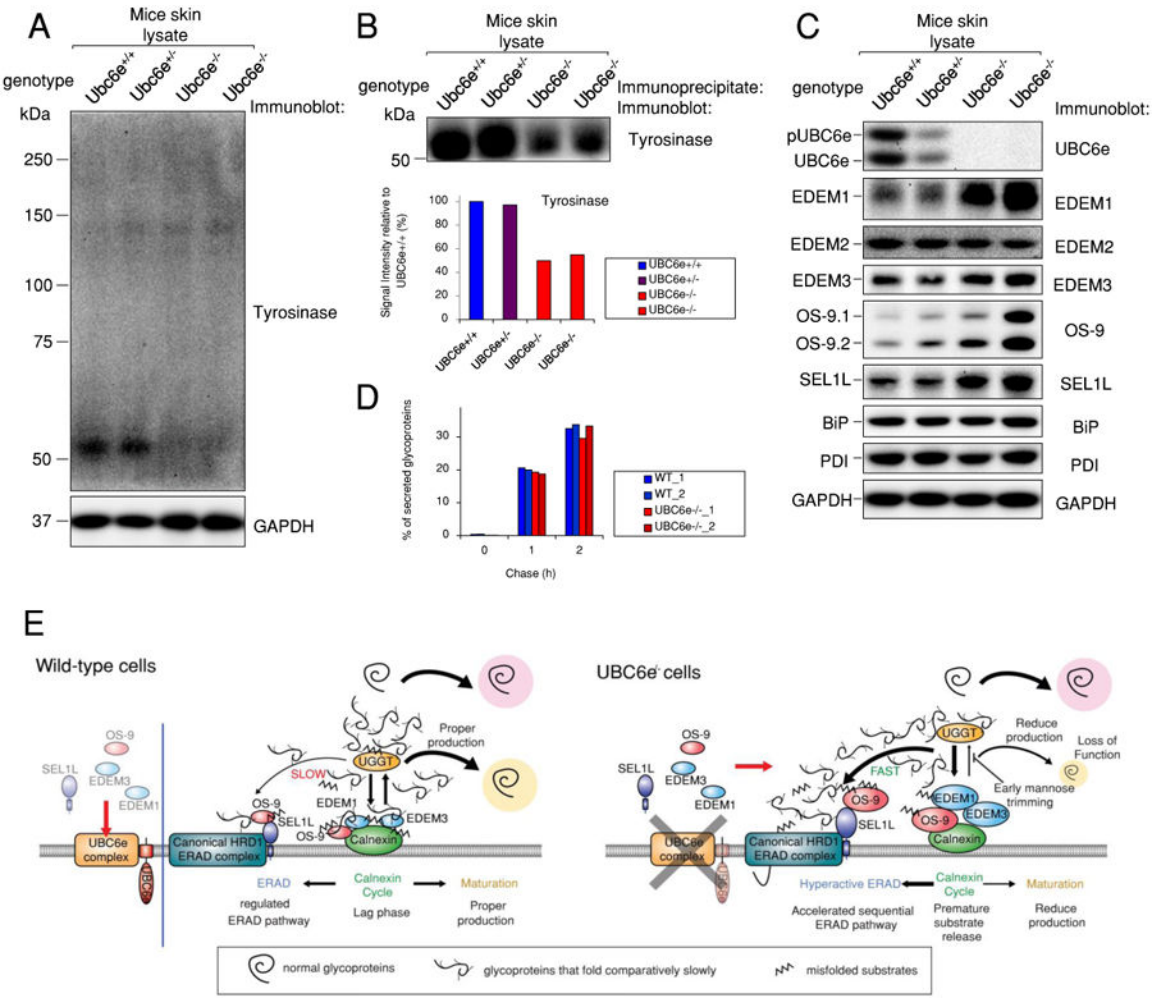

Figure 7. UBC6e regulates ERAD activity through ERAD enhancers to curtail premature destruction of proteins that fold comparatively slowly

(A) Immunoblot of endogenous tyrosinase in skin samples from UBC6e$^{+/+}$, UBC6e$^{+/-}$ and UBC6e$^{-/-}$ mice failed to yield detectable signal. Epidermis of individual mice was homogenized and lysed in 1% NP40. Post-nuclear supernatants were used as the source of skin lysates. 15 μg total protein were separated on SDS-PAGE and immunoblotted for tyrosinase and GAPDH.

(B) UBC6e$^{-/-}$ mice show reduced level of endogenous tyrosinase. 500 μg skin lysate in (A) were immunoprecipitated with antibody to tyrosinase. The recovered tyrosinase was then detected by immunoblotting using the same antibody.

(C) ERAD enhancers are selectively up-regulated in skin lysates from UBC6e$^{-/-}$ mice.

(D) UBC6e deletion does not affect the overall secretion of glycoproteins. Two independently derived wild-type and UBC6e$^{-/-}$ MEFs were pulse-labeled with ^{35}S-Met/Cys for 10 min and chased for the indicated periods. Cell lysates and media were precipitated with Concanavalin A sepharose beads to recover the bulk of glycoproteins. The recovered samples were examined by SDS-PAGE/fluorography. The percentage of secreted glycoproteins was calculated by dividing the signal intensity in the media by the total signal in both the cells and media at that time point.

(E) Model on how UBC6e fine-tunes ERAD activity to achieve a balance between productive folding and degradation. In UBC6e$^{-/-}$ cells, the UBC6e-dependent pathway that constantly down-regulates ERAD enhancers is shut off and ERAD enhancers accumulate. The high-mannose glycans on substrates captured by CNX/CRT are more rapidly trimmed off by the excess ER mannosidases, EDEM1 and EDEM3. After formation of MAN_{5-7}-carrying glycans, the substrates are released from the productive folding cycle on CNX, transferred to OS-9, and then SEL1L in the HRD1 complex for ubiquitination and degradation. The decreased time spent in a productive folding cycle may have little effect on most glycoproteins, but could be detrimental to those that fold comparatively slowly, leading to their loss-of-function.

See also Figure S7.